crystals

MDPI

Article

One-Step Preparation of Si-Doped Ultra-Long β-Ga_2O_3 Nanowires by Low-Pressure Chemical Vapor Deposition

Minglei Tang [1], Guodong Wang [1], Songhao Wu [2,*] and Yang Xiang [1,*]

[1] School of Physics and Electronic Information, Henan Polytechnic University, Jiaozuo 454003, China; tangml136@163.com (M.T.)
[2] School of Integrated Circuits and Electronics, MIIT Key Laboratory for Low-Dimensional Quantum Structure and Devices, Beijing Institute of Technology, Beijing 100081, China
* Correspondence: songhao.wu@bit.edu.cn (S.W.); xiangyang@hpu.edu.cn (Y.X.)

Abstract: In this work, we prepared ultra-long Si-doped β-Ga_2O_3 nanowires on annealed Al_2O_3-film/Si substrate by low-pressure chemical vapor deposition (LPCVD) assisted by Au as catalyst. The length of nanowires exceeds 300 µm and diameters range from ~30 to ~100 nm in one-dimensional structures. The nanowires show good crystal quality and exhibit (201) orientation, confirmed by transmission electron microscopy and X-ray diffraction analysis. The PL spectrum obtained from these β-Ga_2O_3 nanowires has three obvious blue luminescence peaks at 398 nm (3.12 eV), 440 nm (2.82 eV), and 492 nm (2.51 eV). The electrical properties obtained from Si-doped β-Ga_2O_3 nanowires exhibit good conductivity. A metal-semiconductor-metal device is made by using Ti/Au as the electrode, and the device current reaches 200 pA at a bias voltage of 3 V. Our results show that ultra-long Si-doped β-Ga_2O_3 nanowires can be grown directly on the surface of Al_2O_3-film/Si substrates. These nanowires have a very high length-diameter ratio and good electrical properties. A possible mechanism for Si doping is also presented.

Keywords: Si-doped β-Ga_2O_3; nanowires; LPCVD

check for updates

Citation: Tang, M.; Wang, G.; Wu, S.; Xiang, Y. One-Step Preparation of Si-Doped Ultra-Long β-Ga_2O_3 Nanowires by Low-Pressure Chemical Vapor Deposition. *Crystals* **2023**, *13*, 898. https://doi.org/10.3390/cryst13060898

Academic Editor: Vladimir M. Kaganer

Received: 27 April 2023
Revised: 24 May 2023
Accepted: 27 May 2023
Published: 31 May 2023

Copyright: © 2023 by the authors. Licensee MDPI, Basel, Switzerland. This article is an open access article distributed under the terms and conditions of the Creative Commons Attribution (CC BY) license (https://creativecommons.org/licenses/by/4.0/).

1. Introduction

β-Ga_2O_3 has been emerging an important wide bandgap (4.9 eV) semiconductor material [1–6], and has attracted much attention with its outstanding properties, including high breakdown field (~8 MV/cm) [7,8], high Baliga's figure of merit, which is 10 and 4 times higher than that of SiC and GaN [9,10], and thermal and mechanical stability [11–14]. These allow β-Ga_2O_3 to be used in high-power, solar-blind ultraviolet photodetectors, and gas sensors [15,16]. There are five phases of gallium oxide, which are α, β, γ, δ, and ε. Among these phases, β-Ga_2O_3 belongs to the Monoclinic and is the most stable, and the other phases will transform into β-phase gallium oxide at different environments [17]. The space group of β-Ga_2O_3 is C2/m, and lattice constants are a = 12.23 Å, b = 3.04 Å, c = 5.8 Å, $\alpha = \beta = 90°$, $\gamma = 103.8°$ [18,19]. Each unit cell of β-Ga_2O_3 contains two gallium atoms in different positions, denoted as Ga (I) and Ga (II), These atoms are surrounded by oxygen atoms to form a regular tetrahedron or a regular octahedron, and the oxygen atom has three different positions, namely O (I), O(II.), O(III), where two oxygen atoms show triangular coordination and one oxygen atom tetrahedron coordination. Because of the different positions of gallium atoms and oxygen atoms, Ga_2O_3 has appeared as anisotropic in its optical, electrical, and thermal properties [20].

In addition, compared with other wide bandgap semiconductors, β-Ga_2O_3 single crystal has a lower large-scale growth cost, can be grown by the melt method, such as the direct pull methods which have been used for the growth of single crystal silicon, and the mold inverted method, etc. [21–23].

Compared to film and buck β-Ga_2O_3, the controllable growth of β-Ga_2O_3 nanowires is interesting, due to the fact that one-dimensional (1D) circular β-Ga_2O_3 nanowires (NWs)

offer an option to be used as conducting channels, thus achieving further scaling down and ultra-compact electronic integration [24]. For example, Guangming Qu et al. [7] fabricate field-effect transistors (FET) with a back-gate structure, based on β-Ga_2O_3 nanowires transferred to silicon substrate, which has a layer of naturally oxidized silicon oxide on the surface. The switching ratio of the device exceeds 10^8, and the leakage current is only 7.34 fA. These figures indicate that FET based β-Ga_2O_3 nanowires have small dark currents and large switching ratios. Siyuan Xu et al. [8] made a high preferment fin field-effect transistor (FinFET) based on β-Ga_2O_3 nanowire on silicon substrate, and the switching ratio of their device reaches ~4 $\times$ 10^8, and it has a relatively low subthreshold swing (~110 mV), The leakage current is only 4 fA and reaches the limit of the sensing system. The result shows that FinFET based on β-Ga_2O_3 nanowires is comparable with the best reported β-Ga_2O_3 nanowires based on homogeneous epitaxial films, showing the excellent performance of nanowire-based devices.

The one-dimensional material has a high body-to-surface ratio, which is very suitable for detector applications [25–27]. Shan Li et al. [28] constructed high-performance solar blind detectors based on n-Ga_2O_3/p-CuSCN core-shell structure nanowire heterojunction. At the bias voltage of 5 V, the dark current of the device is only 1.03 pA, and photo-to-dark current ratio of 4.14 $\times$ 10^4; moreover, the device is highly sensitive to the weak, deep ultraviolet signal (1.5 $\mu W/cm^2$) and has high-resolution detection. Under illumination with 254 nm light at 5 V, the photodetector has a responsivity of 13.3 mA/W, detectivity of 9.43 $\times$ 10^{11} Jones, and fast response speed, with a rise time of 62 ms and decay time of 35 ms. Shunli Wang et al [29]. used a vertical structure nanorod array to fabricate a solar blind detector, and the device shows good self-energy supply characteristics. At the bias of 0 V, under 254 nm illumination with a light density of 1.2 mW/cm^2, the responsivity of the device is 10.8 mA/W and the optical response time is 0.38 s.

We have also made field emission devices with high performance based on MOCVD grown β-Ga_2O_3 nanowires; the SEM image of the device and its electrical properties are shown in Figure S1 (see Supplementary Materials) [30]. This shows that β-Ga_2O_3 nanowires have great prospects in future integrated applications and vacuum electronics. Since nanowires with larger aspect ratios have better field emission performance and are more in line with the requirements of practical applications, it is necessary to seek nanowires with larger aspect ratios. There have been some methods of preparing Ga_2O_3 nanowires, such as laser pulse deposition (LPD), microwave beam deposition (MBE), Vapor-Liquid-Solid (VLS) [31], metal oxide chemical vapor deposition (MOCVD) [30], and low-pressure chemical vapor deposition (LPCVD) [2].

In this work, we prepared Si-doped β-Ga_2O_3 nanowires by LPCVD using Ga metal and O_2 as precursors. We employed three types of substrate conditions: Si substrate, Al_2O_3-film/Si substrate, and annealed Al_2O_3-film/Si substrate. The β-Ga_2O_3 nanowires were characterized using scanning electron microscopy (SEM), X-ray Photoelectron Spectrum (XPS), X-ray diffraction (XRD), Raman, photoluminescence (PL), and transmission electron microscopy (TEM). The result shows that the β-Ga_2O_3 nanowires grown on the annealed Al_2O_3-film/Si substrate can reach up to 300 μm with a diameter of 30–100 nm, and have a large length-diameter ratio, showing good crystal quality and electrical properties. This provides the foundation for the fabrication of ultra-long nanowire field emission devices to be studied in the future. Additionally, we confirm that the Si element can show out-diffusion toward the surface during annealing of the Al_2O_3-film/Si substrate, resulting in Si-doping. A detailed summary of Ga_2O_3 nanowires reported in the last 5 years can be found in Table 1. In this case, the ultra-long nanowires grown by LPCVD have the highest body surface ratio, the growth method is simpler, and Si doping is introduced, which is comparable to the nanowires grown in recent years in terms of growth process, body surface ratio, and doping. This provides a basis for the preparation of future devices based on β-Ga_2O_3 nanowires.

Table 1. Basic information on Ga_2O_3 nanowires reported the last 5 years.

Year	Substrate	Dopant	L (μm)	D (nm)	Method	References
2017	Si/SiO_2		100		VLS	[32]
2019	Al_2O_3		~100	100–500	VS	[16]
2019	Si/SiO_2			20–100	VLS	[33]
2019	Si	Si	30–70	70–160	LPCVD	[34]
2020	GaAs		10–100	25–40	Oxidation	[35]
2020	Si			50–900	HVPG	[1]
2020	Al_2O_3	Si	>6	50–200	MOCVD	[30]
2021	Al_2O_3		>100	80–300	VLS	[36]
2022	Quartz		30–100	200–1000	Oxidation	[37]
2022	Al_2O_3	Sn	>1000	>1000	CVD	[38]
2022	Si		7–25		CVD	[31]
This work	**Si/Al_2O_3**	**Si**	**>300**	**30–100**	**LPCVD**	

2. Materials and Methods

2.1. Growth of β-Ga_2O_3 Nanowires

The β-Ga_2O_3 nanowires are grown on Si, Al_2O_3-film/Si, and pre-annealed Al_2O_3-film/Si substrate by LPCVD, respectively, as illustrated in Figure 1a. Ga metal (60 μL, purchased from NanJing JinMei Gallium Co., Ltd., Nanjing, China, 99.999%) and high-purity O_2 (5 sccm, 99.999%) are used as precursors. The substrates are sequentially cleaned by acetone, alcohol, and deionized water. First, 4 nm Au films are deposited on the Si and Al_2O_3-film/Si substrates as catalysts, separately, by thermal evaporation deposition. Secondly, the growth process is carried out under low pressure (~12 Pa), and the temperature is set to 900 °C with O_2 flow at 5 sccm, maintained for 10 min. After growth is complete, the samples are naturally cooled for 5 h to room temperature and taken out from the LPCVD, as shown in Figure 1b. Subsequently, to obtain higher length-diameter Ga_2O_3 nanowires, Al_2O_3-film/Si substrate with 4 nm Au film is annealed at 1000 °C for 1 h under ambient O_2. During annealing, the Au film shrinks into small particles, the amorphous Al_2O_3 film becomes partially crystallized, and the Si element of the substrate penetrates through the Al_2O_3 film out-diffusion toward the surface.

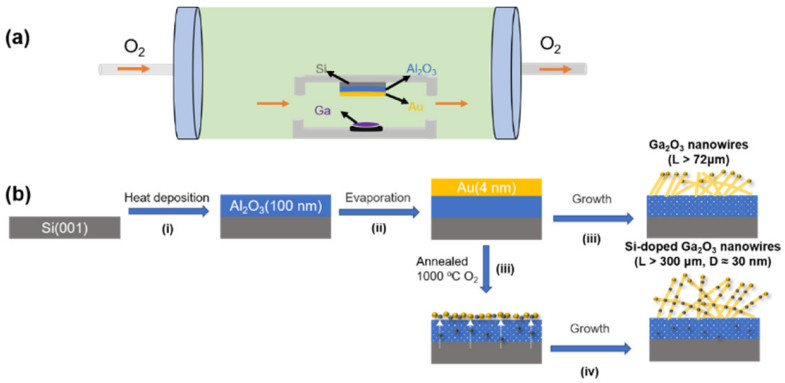

Figure 1. (**a**) Schematic diagram of the precursors, annealed Al_2O_3-film/Si, and LPCVD system. (**b**) The growth process of Ga_2O_3 nanowires.

2.2. Characterization Methods

The nanowires were measured by SEM, XRD, XPS, Raman, PL, and STEM. The SEM investigations are carried out with a Hitachi S-4800 scanning electron microscope. The nanowires are characterized by X-ray diffraction to confirm their crystalline structure in Bede X-ray Metrology (40 kV, λ: ~1.54 Å). The Raman shifts and PL are performed using HORIBA Scientific. A 532 nm green laser is used as the excitation source for the Raman, and a 325 nm blue laser is used as the excitation source for the PL measurement. The I-V

characteristics of the nanowires are measured by Keithley 4200A-SCS (Keithley Instruments, Cleveland, OH, USA).

3. Results and Discussion

As shown in Figure 2a,b, Ga_2O_3 nanowires, which grow on Si and Al_2O_3-film/Si substrates at the same condition, are obtained. In Figure 2a, the nanowires grown on silicon substrates are very dense and most have smaller diameters and shorter lengths of about 10 μm. However, the nanowires grown on Al_2O_3-film/Si substrates are longer, as shown in Figure 2b. In order to measure the length of these nanowires more comprehensively, Figure 2c presents a low magnification SEM image, which shows that the length of the nanowires can reach up to 72 μm, far longer than that of the nanowires grown on silicon substrates. Similar results have also been reported by Abdullah et al. when they prepared Ga_2O_3 nanowires on Si and AlN-film/Si substrate [39]. This might be due to the large lattice mismatch between Si substrates and Ga_2O_3, resulting in a shorter length of Ga_2O_3 nanowires. The amorphous Al_2O_3 film can provide stress-free growth, so the nanowires grown on the Al_2O_3 film are longer. In addition, Au particles are found at the tip of the nanowires grown on both types of substrates and the size of the Au particle is almost the same as the diameter of the nanowires, as shown in Figure 2d,e, indicating that the growth of nanowires is catalyzed by Au [30].

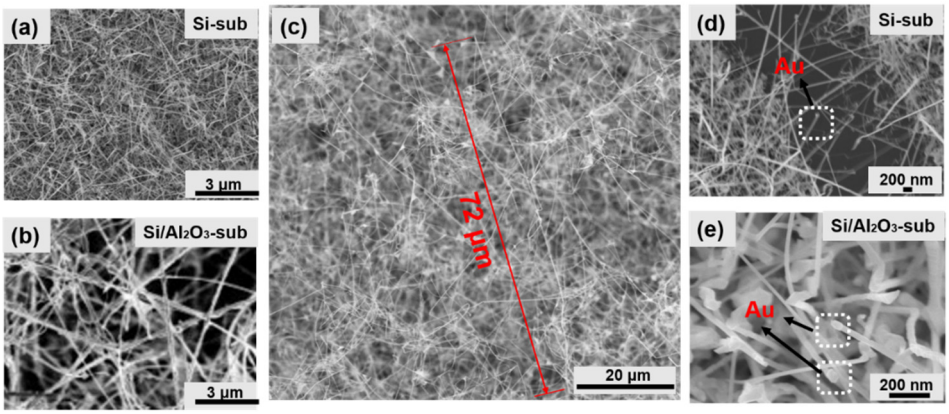

Figure 2. Morphology of the nanowires grown on (**a**) Si substrates and (**b**) Al_2O_3-film/Si substrates. (**c**) Low magnification SEM image of nanowires grown on Al_2O_3-film/Si substrates. (**d**) Au nanocrystals as catalysts while sitting on β-Ga_2O_3 nanorods grown on Si substrates. (**e**) Au nanocrystals as catalysts while sitting on β-Ga_2O_3 nanorods grown on Al_2O_3-film/Si substrates.

The longer the nanowire, the higher its practical value. Therefore, the following will analyze the performances of nanowires grown on Al_2O_3-film/Si substrates. Figure 3a shows the XRD pattern of the Ga_2O_3 nanowires grown on Al_2O_3-film/Si substrates. Except for the Si (100), all the other diffractions can be attributed to β-Ga_2O_3 (PDF# 43-1012). The results indicate that the nanowires are composed of single crystalline β-Ga_2O_3 along (201) orientation. Further analysis of the crystal structure and lattice defects of the β-Ga_2O_3 nanowires was conducted using Raman spectroscopy and photoluminescence measurement. Figure 3b shows the typical phonon modes of β-Ga_2O_3 nanowires (A_1–A_{10}), indicating those nanowires belong to β phase structure, and the sharp Raman peak of A_3 also implies high crystallinity of nanowires. Figure 3c shows the room-temperature PL spectrum of β-Ga_2O_3 nanowires. Orange is the original map, after peaking, there are three obvious blue luminescence peaks of Ga_2O_3 nanowires at 398 nm (3.12 eV), 440 nm (2.82 eV), and 492 nm (2.51 eV). The luminescence peaks of Ga_2O_3 nanowires are always electron transitions caused by intrinsic defect energy levels and impurity levels. The intrinsic defect is always attributed to gallium vacancies (V_{Ga}), oxygen vacancies (V_O), and the gallium-oxygen vacancy pair (V_{Ga} + V_O). The impurities defect, in this work, is due to Au and Si (detailed discussion in the TEM section), but they would not excite PL, because they have

shallow donor levels [40]. The blue PL is attributed to donor–acceptor recombination [41]. The Si is a shallow donor, and V_{Ga} or the divacancy V_{Ga} + V_O has been suggested as the responsible acceptor, indicating that there is a significant amount of V_{Ga} or V_{Ga} + V_O on the surface of the nanowires [42].

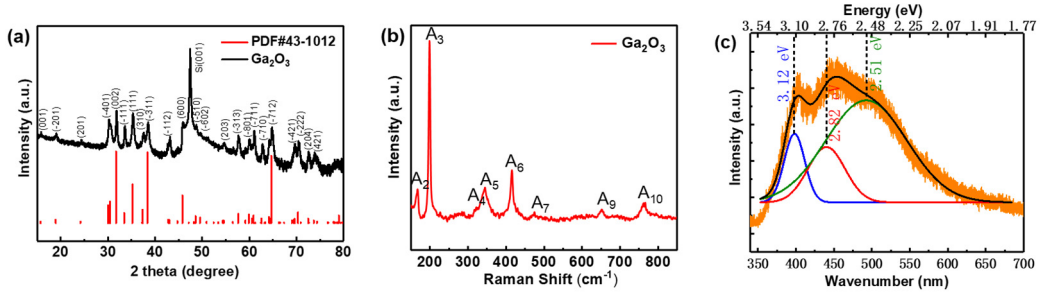

Figure 3. (**a**) X-ray diffraction (XRD), (**b**) Raman, and (**c**) room temperature photoluminescence (PL) spectra of β-Ga_2O_3 nanowires grown on Al_2O_3-film/Si substrates.

To further study the composition and chemical state of the elements in the β-Ga_2O_3 nanowires, XPS characterization was performed, as shown in Figure 4. The binding energy scale has referenced the C 1s core level (284.8 eV). The characteristic peaks of Ga and O are clearly observed (Figure 4a), including Ga 3d, Ga 3p, Ga 3s, O 1s, Ga 2p, and Ga LMM, O KLL. This proves that the samples are composed of the above elements, coinciding well with the XRD testing results. The Ga 2p1 and 2p3 are located at 1144 eV and 1117 eV, respectively, and the interval between Ga 2p1 and 2p3 peaks is approximately 27.0 eV, as shown in Figure 4b, which indicates the presence of Ga_2O_3 [43].

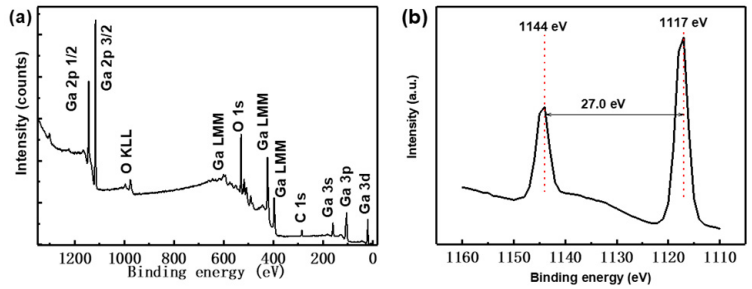

Figure 4. XPS spectra of β-Ga_2O_3 nanowires grown on Al_2O_3-film/Si substrates: (**a**) survey, (**b**) Ga 2p.

In order to further increase the length of the nanowire, pre-annealing treatment is performed on Al_2O_3-film/Si substrates in oxygen, the process carried out under low pressure (~12 Pa), with temperature set to 900 °C, with O_2 flow 5 sccm, for 1 h. under the same growing conditions (low pressure (~12 Pa)), a temperature of 900 °C and O_2 flow of 5 sccm, for 10 min. Ultra-long Ga_2O_3 nanowires are obtained with lengths exceeding 300 μm and a diameter of 30–100 nm, as shown in Figure 5a,b. The growth time of Ga_2O_3 nanoparticles is 10 min, so the growth rate is up to 30 μm/min. It was noted that the density of nanowires is lower than the above-mentioned nanowires, which grow on Si and Al_2O_3-film/Si substrate, due to fewer nucleation sites, because the Al_2O_3 film becomes partly crystallized after annealing. The microstructure and compositional distribution of the nanowires were further investigated by STEM (under ultra-high vacuum (<10^{-10} Torr) at an accelerating voltage of 10 kV) and EDX mapping. As shown in Figure 5c, all atoms are arranged neatly, without obvious dislocation or surface point defect. From its diffraction pattern, its diffraction spots are bright and ordered, indicating that nanowires have high quality. We measured the surface atomic layer spacing, which is 0.559 nm, corresponding to the (001) plane of β-Ga_2O_3, indicating that the nanowires grow along the shortest b-axis. Because, during crystal growth, the density of the crystal surface is higher and the lattice is more stable in the shortest axis, the growth speed in the short axis direction is

fastest (Figure 5e). Figure 5d shows STEM-energy dispersive X-ray (STEM-EDX) elemental mapping of Ga, O, Au, and Si. The Au elements should be introduced from the Au particles, and the Si elements are introduced from the out-diffusion of Si substrate during annealing at 1000 °C. Corresponding EDX spectra and atomic quantification are shown in Figure 5f.

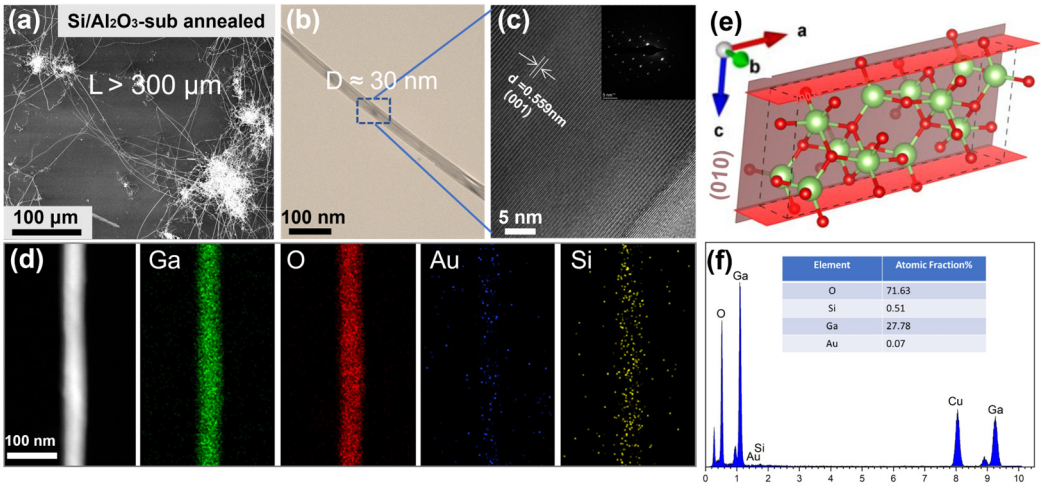

Figure 5. (**a**) The SEM image, (**b**) the HRTEM, and (**c**) the atomic resolution TEM of ultra-long Ga_2O_3 nanowires. (**d**) HAADF image and the corresponding EDS mapping of Ga, O, Si and Au of Ga_2O_3 nanowires on annealed Al_2O_3-film/Si substrates. (**e**) Crystal structure of ultra-long Ga_2O_3 nanowires. (**f**) EDX area scan spectra and atomic quantification of ultra-long Ga_2O_3 nanowires.

To further study the growth mechanism of nanowires, the unannealed and annealed Al_2O_3-film/Si substrates were further investigated by TEM, and the results are shown in Figure 6a,d. The unannealed substrate has three distinct layers: Si (001), SiO_2(~7 nm), and Al_2O_3 film (~100 nm). The thin layer of SiO_2 is formed by the natural oxidation of the Si substrate surface. The spot diffraction spectrum shows that the Al_2O_3 film is amorphous (Figure 6b). From the associated EDX mapping (Figure 6c), it can be seen that all Si elements only exist under the Al_2O_3 film. Interestingly, after annealing, the amorphous Al_2O_3 layer becomes denser and partially crystallized (Figure 6d). Its diffraction spectrum has also changed from a blurred ring to the coexistence of diffraction spots and rings, also indicating that the partial Al_2O_3 is crystallized. It was also observed that the Si element penetrated the Al_2O_3 film out diffusion toward the surface, which can be seen from the dashed square of Figure 6f, resulting in Si-doping in the β-Ga_2O_3 nanowires. Figure 6g shows the EDX spot scan spectra of Ga_2O_3 nanowires grown on unannealed Al_2O_3-film/Si substrate; the corresponding area is shown in Figure S2a, the results showing that only gallium and oxygen elements can be detected, which indicates that the presence of Al_2O_3 film reduces the Si element in the grown Ga_2O_3 nanowire, and the Au element is not measured, because the nanowire length is higher, the density is large, and the proportion of gold element is too small to be detected. Figure 6h is the EDX spot scan spectra of the ultra-long gallium oxide nanowire grown on annealed Al_2O_3-film/Si substrate; the corresponding area is shown in Figure S2b, and we can see the presence of Ga, O, Au, and Si signals. Since the diameter of the nanowires is much smaller than the scanning range of the EDX spot scan, the measured elemental weight ratio is not accurate, but the presence of a large number of Si elements further confirms that the silicon element of the substrate diffuses to the surface of the substrate after oxygen annealing, supporting the conclusion in Figure 6a–f.

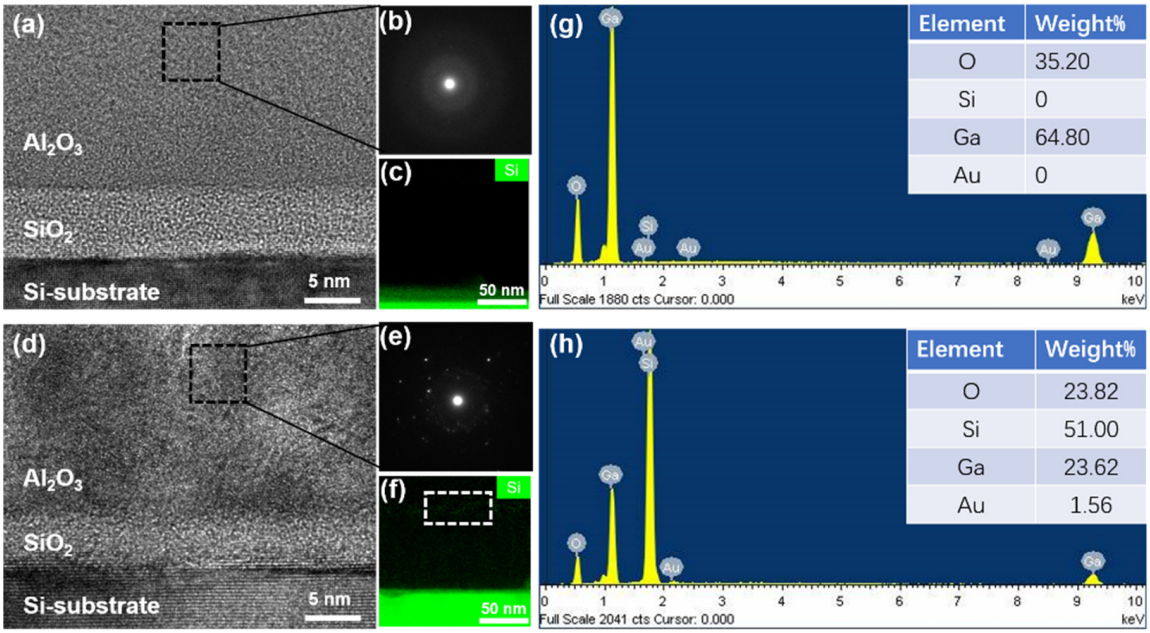

Figure 6. The Cross-section (**a**,**d**) TEM, (**b**,**e**) diffraction pattern, and (**c**,**f**) associated EDS mapping of the unannealed and annealed Al_2O_3-film/Si substrate. EDX spot scan spectra (**g**,**h**) of Ga_2O_3 nanowires on unannealed and annealed Al_2O_3-film/Si substrates, respectively.

To characterize the conductivity characteristics of the obtained β-Ga_2O_3 NWs, two electrodes with a width of 2 µm were prepared at both ends of the nanowires using standard photolithography techniques, which are shown in Figure 7a. As a bridge, the single nanowire connected the two Ti/Au electrodes. The I-V characteristic of the NWs was measured by Keithley 4200A-SCS with a step of 0.5 V, varying the source voltage from −3 V to 3 V at room temperature. The corresponding current values are shown in Figure 7b. The graph is non-linear and resembles the curve of a Schottky diode, which is between the conductor and semiconductor layer. The current reached 200 pA at 3 V and its resistivity is ~4 kΩ·cm, exhibiting good conductivity [44].

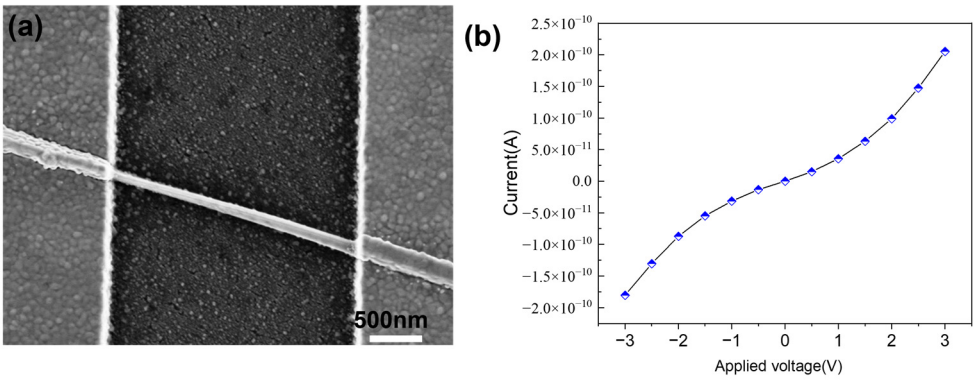

Figure 7. (**a**) The SEM image of the Ga_2O_3 nanowires with electrodes. (**b**) I-V curve of ultra-long β-Ga_2O_3 nanowires.

4. Conclusions

The growth of Ga_2O_3 nanowires on Si, Al_2O_3-film/Si, and annealed Al_2O_3-film/Si substrate by LPCVD was realized. The ultra-long nanowires can be prepared on the annealed Al_2O_3-film/Si substrate. By annealing the Al_2O_3-film/Si substrate, the amorphous Al_2O_3 film becomes partially crystallized, resulting in the nucleation sites being reduced, thus nanowires on the annealed Al_2O_3-film/Si substrate are sparser than others. The length

of nanowires is more than 300 μm and the diameter is about 30–100 nm. Through XRD, XPS, and Raman, we determined that the Ga_2O_3 nanowire belongs to the monoclinic β phase. The nanowire shows high crystal quality and grows along the b-axis because this axis has the lowest epitaxial potential energy. The two kinds of dopants, Au and Si, are confirmed by the associated EDX mapping, the Si-doping resulting from the Si substrate. The nanowire also shows good conductivity, and its current can reach 200 pA at 3 V. This work provides a novel means of growing high body-to-surface ratio β-Ga_2O_3 nanowires, which is promising for applications including power electronics, solar-blind photodetection, and gas sensors. Future work includes growth studies with the aim of increasing the density of ultra-long β-Ga_2O_3 nanowires, fabricating field emission device based ultra-long β-Ga_2O_3 nanowires, and exploring a method of increasing the length of ultra-long β-Ga_2O_3 nanowires.

Supplementary Materials: The following supporting information can be downloaded at: https://www.mdpi.com/article/10.3390/cryst13060898/s1. Figure S1: (a) field emissions device based on β-Ga_2O_3 nanowires (b) electrical properties of field emission device. Figure S2: EDX spot scan area of (a) Ga_2O_3 nanowires grown on an unannealed Al_2O_3-film/Si substrate (b) ultra-long nanowires grown on annealed Al_2O_3-film/Si substrate.

Author Contributions: M.T.: experiment, data processing and analyzing, manuscript writing, review, and editing. S.W., G.W.: analyzing, manuscript review editing, and supervision. Y.X.: supervision and Funding acquisition. All authors have read and agreed to the published version of the manuscript.

Funding: National natural science foundation of China (No 62173128).

Data Availability Statement: The data that support the findings of this study are available from the corresponding author upon reasonable request.

Conflicts of Interest: The authors declare no conflict of interest.

References

1. dela Torre, H.M.B.; Santos, G.N.C. Synthesis and Characterization of Monoclinic Gallium Oxide Nanomaterials for High-Concentration Ethanol Vapor Detection. *IOP Conf. Ser. Mater. Sci. Eng.* **2020**, *739*, 012031. [CrossRef]
2. Han, N.; Wang, F.; Yang, Z.; Yip, S.; Dong, G.; Lin, H.; Fang, M.; Hung, T.; Ho, J.C. Low-temperature growth of highly crystalline beta-Ga_2O_3 nanowires by solid-source chemical vapor deposition. *Nanoscale Res. Lett.* **2014**, *9*, 347. [CrossRef] [PubMed]
3. Zhao, X.; Cui, W.; Wu, Z.; Guo, D.; Li, P.; An, Y.; Li, L.; Tang, W. Growth and Characterization of Sn Doped β-Ga_2O_3 Thin Films and Enhanced Performance in a Solar-Blind Photodetector. *J. Electron. Mater.* **2017**, *46*, 2366–2372. [CrossRef]
4. Li, S.; Zhi, Y.; Lu, C.; Wu, C.; Yan, Z.; Liu, Z.; Yang, J.; Chu, X.; Guo, D.; Li, P.; et al. Broadband Ultraviolet Self-Powered Photodetector Constructed on Exfoliated beta-Ga_2O_3/CuI Core-Shell Microwire Heterojunction with Superior Reliability. *J. Phys. Chem. Lett.* **2021**, *12*, 447–453. [CrossRef] [PubMed]
5. Li, P.; Shi, H.; Chen, K.; Guo, D.; Cui, W.; Zhi, Y.; Wang, S.; Wu, Z.; Chen, Z.; Tang, W. Construction of GaN/Ga_2O_3 p–n junction for an extremely high responsivity self-powered UV photodetector. *J. Mater. Chem. C* **2017**, *5*, 10562–10570. [CrossRef]
6. Jia, M.; Wang, F.; Tang, L.; Xiang, J.; Teng, K.S.; Lau, S.P. High-Performance Deep Ultraviolet Photodetector Based on NiO/beta-Ga_2O_3 Heterojunction. *Nanoscale Res. Lett.* **2020**, *15*, 47. [CrossRef]
7. Qu, G.; Xu, S.; Liu, L.; Tang, M.; Wu, S.; Jia, C.; Zhang, X.; Song, W.; Lee, Y.J.; Xu, J.; et al. Single β-Ga_2O_3 nanowire back-gate field-effect transistor. *Semicond. Sci. Technol.* **2022**, *37*, 085009. [CrossRef]
8. Xu, S.; Liu, L.; Qu, G.; Zhang, X.; Jia, C.; Wu, S.; Ma, Y.; Lee, Y.J.; Wang, G.; Park, J.-H.; et al. Single β-Ga_2O_3 nanowire based lateral FinFET on Si. *Appl. Phys. Lett.* **2022**, *120*, 153501. [CrossRef]
9. Guo, D.-Y.; Li, P.-G.; Chen, Z.-W.; Wu, Z.-P.; Tang, W.-H. Ultra-wide bandgap semiconductor of beta-Ga_2O_3 and its research progress of deep ultraviolet transparent electrode and solar-blind photodetector. *Acta Phys. Sin.* **2019**, *68*, 078501. [CrossRef]
10. Qin, Y.; Long, S.; Dong, H.; He, Q.; Jian, G.; Zhang, Y.; Hou, X.; Tan, P.; Zhang, Z.; Lv, H.; et al. Review of deep ultraviolet photodetector based on gallium oxide. *Chin. Phys. B* **2019**, *28*, 018501. [CrossRef]
11. Pearton, S.J.; Yang, J.; Cary, P.H.; Ren, F.; Kim, J.; Tadjer, M.J.; Mastro, M.A. A review of Ga_2O_3 materials, processing, and devices. *Appl. Phys. Rev.* **2018**, *5*, 011301. [CrossRef]
12. Zhang, X.; Wang, L.; Wang, X.; Chen, Y.; Shao, Q.; Wu, G.; Wang, X.; Lin, T.; Shen, H.; Wang, J.; et al. High-performance β-Ga_2O_3 thickness dependent solar blind photodetector. *Opt. Express* **2020**, *28*, 4169–4177. [CrossRef]
13. Guo, D.; Wu, Z.; Li, P.; An, Y.; Liu, H.; Guo, X.; Yan, H.; Wang, G.; Sun, C.; Li, L.; et al. Fabrication of β-Ga_2O_3 thin films and solar-blind photodetectors by laser MBE technology. *Opt. Mater. Express* **2014**, *4*, 1067–1076. [CrossRef]
14. Wu, H.; Huang, Y.; Zhi, Y.; Wang, X.; Chu, X.; Chen, Z.; Li, P.; Wu, Z.; Tang, W. Single-layer graphene electrode enhanced sensitivity and response speed of β-Ga_2O_3 solar-blind photodetector. *Opt. Mater. Express* **2019**, *9*, 1394–1403. [CrossRef]

15. Tak, B.R.; Garg, M.; Dewan, S.; Torres-Castanedo, C.G.; Li, K.-H.; Gupta, V.; Li, X.; Singh, R. High-temperature photocurrent mechanism of β-Ga_2O_3 based metal-semiconductor-metal solar-blind photodetectors. *J. Appl. Phys.* **2019**, *125*, 144501. [CrossRef]
16. Xie, C.; Lu, X.T.; Ma, M.R.; Tong, X.W.; Zhang, Z.X.; Wang, L.; Wu, C.Y.; Yang, W.H.; Luo, L.B. Catalyst-Free Vapor–Solid Deposition Growth of β-Ga_2O_3 Nanowires for DUV Photodetector and Image Sensor Application. *Adv. Opt. Mater.* **2019**, *7*, 1901257. [CrossRef]
17. Mastro, M.A.; Kuramata, A.; Calkins, J.; Kim, J.; Ren, F.; Pearton, S.J. Perspective—Opportunities and Future Directions for Ga_2O_3. *ECS J. Solid State Sci. Technol.* **2017**, *6*, P356–P359. [CrossRef]
18. Peng, Y.; Zhang, Y.; Chen, Z.; Guo, D.; Zhang, X.; Li, P.; Wu, Z.; Tang, W. Arrays of Solar-Blind Ultraviolet Photodetector Based on β-Ga_2O_3 Epitaxial Thin Films. *IEEE Photonics Technol. Lett.* **2018**, *30*, 993–996. [CrossRef]
19. Wu, Z.; Jiao, L.; Wang, X.; Guo, D.; Li, W.; Li, L.; Huang, F.; Tang, W. A self-powered deep-ultraviolet photodetector based on an epitaxial Ga_2O_3/Ga:ZnO heterojunction. *J. Mater. Chem. C* **2017**, *5*, 8688–8693. [CrossRef]
20. He, H.; Orlando, R.; Blanco, M.A.; Pandey, R.; Amzallag, E.; Baraille, I.; Rérat, M. First-principles study of the structural, electronic, and optical properties of Ga_2O_3 in its monoclinic and hexagonal phases. *Phys. Rev. B* **2006**, *74*, 195123. [CrossRef]
21. Tao, X. Bulk gallium oxide single crystal growth. *J. Semicond.* **2019**, *40*, 010401. [CrossRef]
22. Fu, B.; Jian, G.; Mu, W.; Li, Y.; Wang, H.; Jia, Z.; Li, Y.; Long, S.; Shi, Y.; Tao, X. Crystal growth and design of Sn-doped β-Ga_2O_3: Morphology, defect and property studies of cylindrical crystal by EFG. *J. Alloys Compd.* **2022**, *896*, 162830. [CrossRef]
23. Yao, Y.; Ishikawa, Y.; Sugawara, Y. Revelation of Dislocations in β-Ga_2O_3 Substrates Grown by Edge-Defined Film-Fed Growth. *Phys. Status Solidi* **2019**, *217*, 1900630. [CrossRef]
24. Zou, X.B.; Xie, D.Y.; Sun, Y.; Wang, C.X. Nanowires mediated growth of beta-Ga_2O_3 nanobelts for high-temperature (>573 K) solar-blind photodetectors. *Nano Res.* **2022**, *2022*, 5548–5554. [CrossRef]
25. Shin, G.; Kim, H.-Y.; Kim, J. Deep-ultraviolet photodetector based on exfoliated n-type β-Ga_2O_3 nanobelt/p-Si substrate heterojunction. *Korean J. Chem. Eng.* **2018**, *35*, 574–578. [CrossRef]
26. Lai, J.; Hasan, M.N.; Swinnich, E.; Tang, Z.; Shin, S.-H.; Kim, M.; Zhang, P.; Seo, J.-H. Flexible crystalline β-Ga_2O_3 solar-blind photodetectors. *J. Mater. Chem. C* **2020**, *8*, 14732–14739. [CrossRef]
27. Yamamura, K.; Zhu, L.; Irvine, C.P.; Scott, J.A.; Singh, M.; Jallandhra, A.; Bansal, V.; Phillips, M.R.; Ton-That, C. Defect Compensation in Nitrogen-Doped β-Ga_2O_3 Nanowires: Implications for Bipolar Nanoscale Devices. *ACS Appl. Nano Mater.* **2022**, *5*, 12087–12094. [CrossRef]
28. Li, S.; Guo, D.; Li, P.; Wang, X.; Wang, Y.; Yan, Z.; Liu, Z.; Zhi, Y.; Huang, Y.; Wu, Z.; et al. Ultrasensitive, Superhigh Signal-to-Noise Ratio, Self-Powered Solar-Blind-Photodetector Based on n-Ga_2O_3/p-CuSCN Core-Shell Microwire Heterojunction. *ACS Appl. Mater. Interfaces* **2019**, *11*, 35105–35114. [CrossRef]
29. Wang, S.; Chen, K.; Zhao, H.; He, C.; Wu, C.; Guo, D.; Zhao, N.; Ungar, G.; Shen, J.; Chu, X.; et al. beta-Ga_2O_3 nanorod arrays with high light-to-electron conversion for solar-blind deep ultraviolet photodetection. *RSC Adv.* **2019**, *9*, 6064–6069. [CrossRef]
30. Jia, C.; Jeon, D.W.; Xu, J.; Yi, X.; Park, J.H.; Zhang, Y. Catalyst-Assisted Large-Area Growth of Single-Crystal beta-Ga_2O_3 Nanowires on Sapphire Substrates by Metal-Organic Chemical Vapor Deposition. *Nanomaterials* **2020**, *10*, 1031. [CrossRef]
31. Yadav, A.; Fu, B.; Bonvicini, S.N.; Ly, L.Q.; Jia, Z.; Shi, Y. β-Ga_2O_3 Nanostructures: Chemical Vapor Deposition Growth Using Thermally Dewetted Au Nanoparticles as Catalyst and Characterization. *Nanomaterials* **2022**, *12*, 2589. [CrossRef]
32. Korbutowicz, R.; Stafiniak, A.; Serafińczuk, J. Ga_2O_3 nanowires preparation at atmospheric pressure. *Mater. Sci.-Pol.* **2017**, *35*, 412–420. [CrossRef]
33. Wang, H.; Wang, Y.; Gong, S.; Zhou, X.; Yang, Z.; Yang, J.; Han, N.; Chen, Y. Growth of Ga_2O_3 Nanowires via Cu-As-Ga Ternary Phase Diagram. *Crystals* **2019**, *9*, 155. [CrossRef]
34. Alhalaili, B.; Vidu, R.; Islam, M.S. The Growth of Ga_2O_3 Nanowires on Silicon for Ultraviolet Photodetector. *Sensors* **2019**, *19*, 5301. [CrossRef]
35. Alhalaili, B.; Mao, H.; Dryden, D.M.; Cansizoglu, H.; Bunk, R.J.; Vidu, R.; Woodall, J.; Islam, M.S. Influence of Silver as a Catalyst on the Growth of β-Ga_2O_3 Nanowires on GaAs. *Materials* **2020**, *13*, 5377. [CrossRef] [PubMed]
36. Krawczyk, M.; Suchorska-Woźniak, P.; Szukiewicz, R.; Kuchowicz, M.; Korbutowicz, R.; Teterycz, H. Morphology of Ga_2O_3 Nanowires and Their Sensitivity to Volatile Organic Compounds. *Nanomaterials* **2021**, *11*, 456. [CrossRef]
37. Alhalaili, B.; Al-Duweesh, A.; Popescu, I.N.; Vidu, R.; Vladareanu, L.; Islam, M.S. Improvement of Schottky Contacts of Gallium Oxide (Ga_2O_3) Nanowires for UV Applications. *Sensors* **2022**, *22*, 2048. [CrossRef] [PubMed]
38. Lu, Y.-C.; Zhang, Z.-F.; Yang, X.; He, G.-H.; Lin, C.-N.; Chen, X.-X.; Zang, J.-H.; Zhao, W.-B.; Chen, Y.-C.; Zhang, L.-L.; et al. High-performance solar-blind photodetector arrays constructed from Sn-doped Ga_2O_3 microwires via patterned electrodes. *Nano Res.* **2022**, *15*, 7631–7638. [CrossRef]
39. Abdullah, Q.N.; Yam, F.K.; Mohmood, K.H.; Hassan, Z.; Qaeed, M.A.; Bououdina, M.; Almessiere, M.A.; Al-Otaibi, A.L.; Abdulateef, S.A. Free growth of one-dimensional β-Ga_2O_3 nanostructures including nanowires, nanobelts and nanosheets using a thermal evaporation method. *Ceram. Int.* **2016**, *42*, 13343–13349. [CrossRef]
40. Rajapitamahuni, A.K.; Thoutam, L.R.; Ranga, P.; Krishnamoorthy, S.; Jalan, B. Impurity band conduction in Si-doped β-Ga_2O_3 films. *Appl. Phys. Lett.* **2021**, *118*, 072105. [CrossRef]
41. Onuma, T.; Saito, S.; Sasaki, K.; Masui, T.; Yamaguchi, T.; Honda, T.; Higashiwaki, M. Valence band ordering in β-Ga_2O_3 studied by polarized transmittance and reflectance spectroscopy. *JPN J. Appl. Phys.* **2015**, *54*, 112601. [CrossRef]
42. Ho, Q.D.; Frauenheim, T.; Deák, P. Origin of photoluminescence in $\beta-Ga_2O_3$. *Phys. Rev. B* **2018**, *97*, 115163. [CrossRef]

43. Zhang, T.; Li, Y.; Feng, Q.; Zhang, Y.; Ning, J.; Zhang, C.; Zhang, J.; Hao, Y. Effects of growth pressure on the characteristics of the β-Ga_2O_3 thin films deposited on (0001) sapphire substrates. *Mater. Sci. Semicond. Process.* **2021**, *123*, 105572. [CrossRef]
44. Oshima, T.; Okuno, T.; Arai, N.; Suzuki, N.; Ohira, S.; Fujita, S. Vertical solar-blind deep-ultraviolet schottky photodetectors based on β-Ga_2O_3 substrates. *Appl. Phys. Express* **2008**, *1*, 011202. [CrossRef]

Disclaimer/Publisher's Note: The statements, opinions and data contained in all publications are solely those of the individual author(s) and contributor(s) and not of MDPI and/or the editor(s). MDPI and/or the editor(s) disclaim responsibility for any injury to people or property resulting from any ideas, methods, instructions or products referred to in the content.